

Electronic Supporting Information

Four [Tp*W(μ_3 -S) $_3$ Cu $_3$ (μ_3 -Br)]-based clusters: synthesis, structural characterization and third-order NLO properties

Xue Lü,^a Xi Chen,^a Zhi-Gang Ren,^a Jian-Ping Lang^{*,a,b} Dong Liu,^a and Zhen-Rong Sun^{*,c}

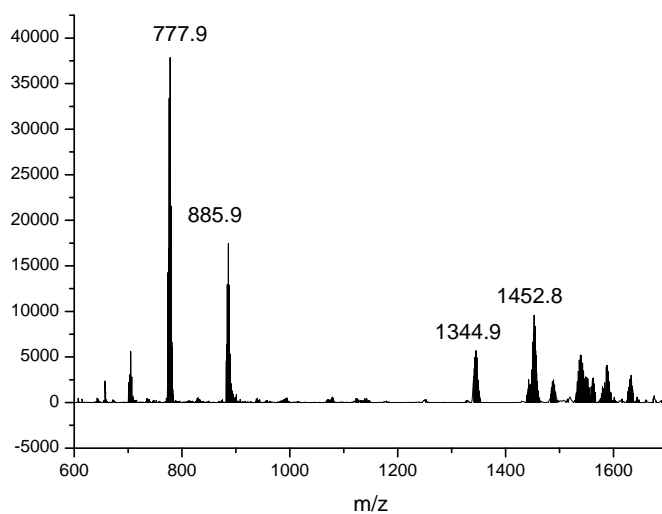
^a College of Chemistry, Chemical Engineering and Materials Science, Soochow University, Suzhou 215123, Jiangsu, P. R. China

^b State Key Laboratory of Coordination Chemistry, Nanjing University, Nanjing 210093, Jiangsu, P. R. China

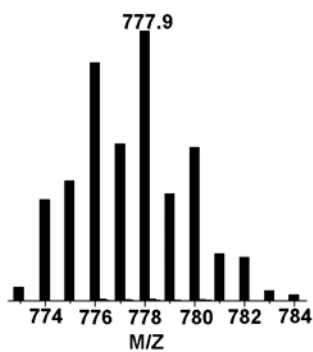
^c Department of Physics, East China Normal University, Shanghai 200062, People's Republic of China

Table of Contents

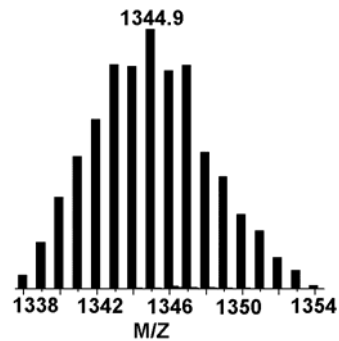
Fig. S1	The positive-ion ESI mass spectrum of 2 in DMF.....	S3
Fig. S2	The positive-ion ESI mass spectrum of 3 in DMF.....	S4
Fig. S3	The negative-ion ESI mass spectrum of 3 in DMF.....	S5
Fig. S4	The positive-ion ESI mass spectrum of 4 in DMF.....	S6
Fig. S5	The positive-ion ESI mass spectrum of 5 in DMF.....	S7
Fig. S6.	View of the arrangement of the cationic chain and the cluster anion of 3 along the <i>bc</i> plane.....	S8
Fig. S7.	View of the 2D network derived from the hydrogen bonding interactions among the MA ligands and MeOH solvent molecules in 4 ·2MeOH.....	S8
Fig. S8.	(a) The H-bonding 1D chain in 5 ·MeCN·0.5Et ₂ O extended along the <i>c</i> axis. (b) The H-bonding 2D network in 5 ·MeCN·0.5Et ₂ O viewed along the <i>ac</i> plane. (c) The 3D H-bound structure in 5 ·MeCN·0.5Et ₂ O looking down the <i>c</i> axis.....	S9
Fig. S9	DFWM signal for the DMF solutions of 2 (a), 4 (b) and 5 (c) with concentrations 5.56×10^{-4} M for 2 , 2.75×10^{-4} M for 4 and 5.54×10^{-4} M for 5 . The black solid squares are experimental data, and the red solid curves are the theoretical fit.....	S10



(a)

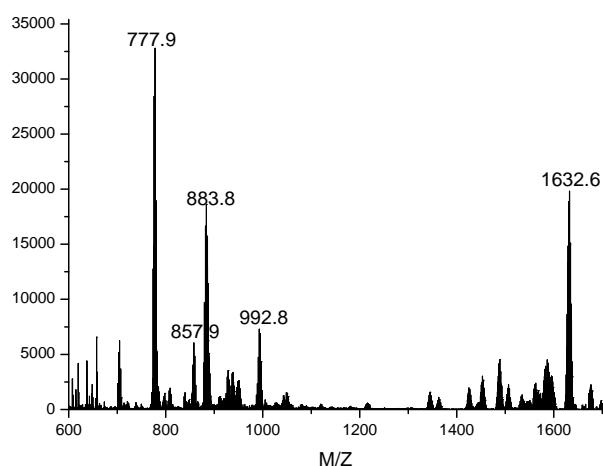


(b)

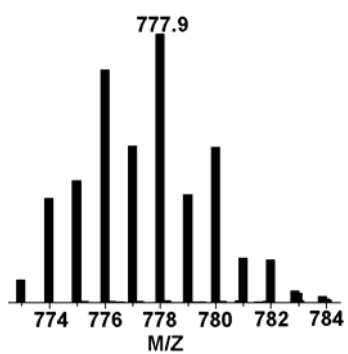


(c)

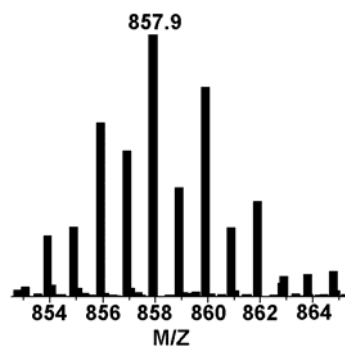
Figure S1. (a) The positive-ion ESI mass spectrum of **2**. (b) View of the observed (dark) and the calculated (gray) isotopic patterns for the $[\{Tp^*WS_3Cu_2\}+DMF]^+$ cation. (c) View of the observed (dark) and the calculated (gray) isotopic patterns for the $[(Tp^*WS_3)_2Cu_3]^+$ cation (c).



(a)

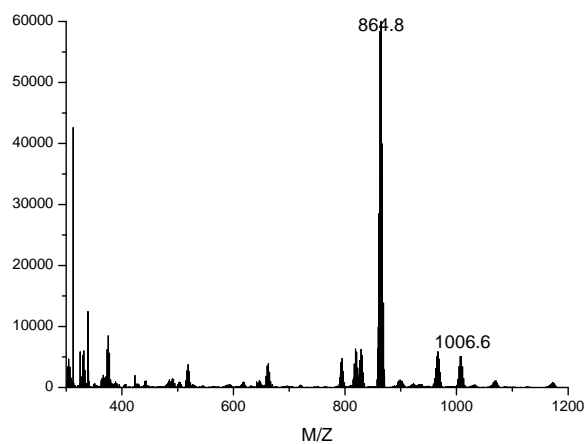


(b)

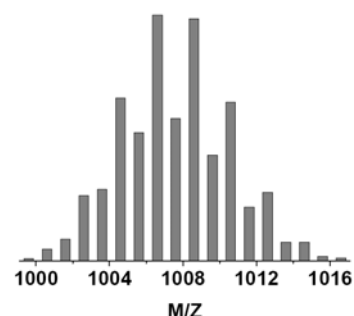
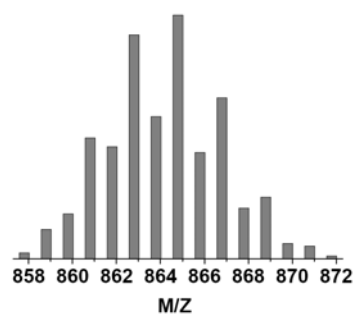
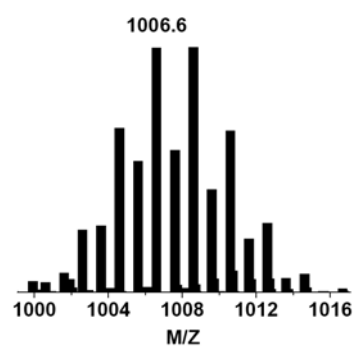
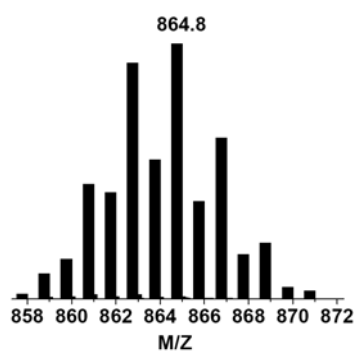


(c)

Figure S2. (a) The positive-ion ESI mass spectrum of **3** in DMF. (b) View of the observed (dark) and the calculated (gray) isotopic patterns for the $[\{\text{Tp}^*\text{WS}_3\text{Cu}_2\}+\text{DMF}]^+$ cation. (c) View of the observed (dark) and the calculated (gray) isotopic patterns for the $[\{\text{Tp}^*\text{WS}_3\text{Cu}_2\text{Br}\}+\text{DMF}+\text{H}]^+$ cation.



(a)



(b)

(c)

Figure S3. (a) The negative-ion ESI mass spectrum of **3** in DMF. (b) View of the observed (dark) and the calculated (gray) isotopic patterns for the $[\text{Tp}^*\text{WS}_3\text{Cu}_2\text{Br}_2]^-$ anion. (c) View of the observed (dark) and the calculated (gray) isotopic patterns for the $[\text{Tp}^*\text{WS}_3\text{Cu}_3\text{Br}_3]^-$ anion.

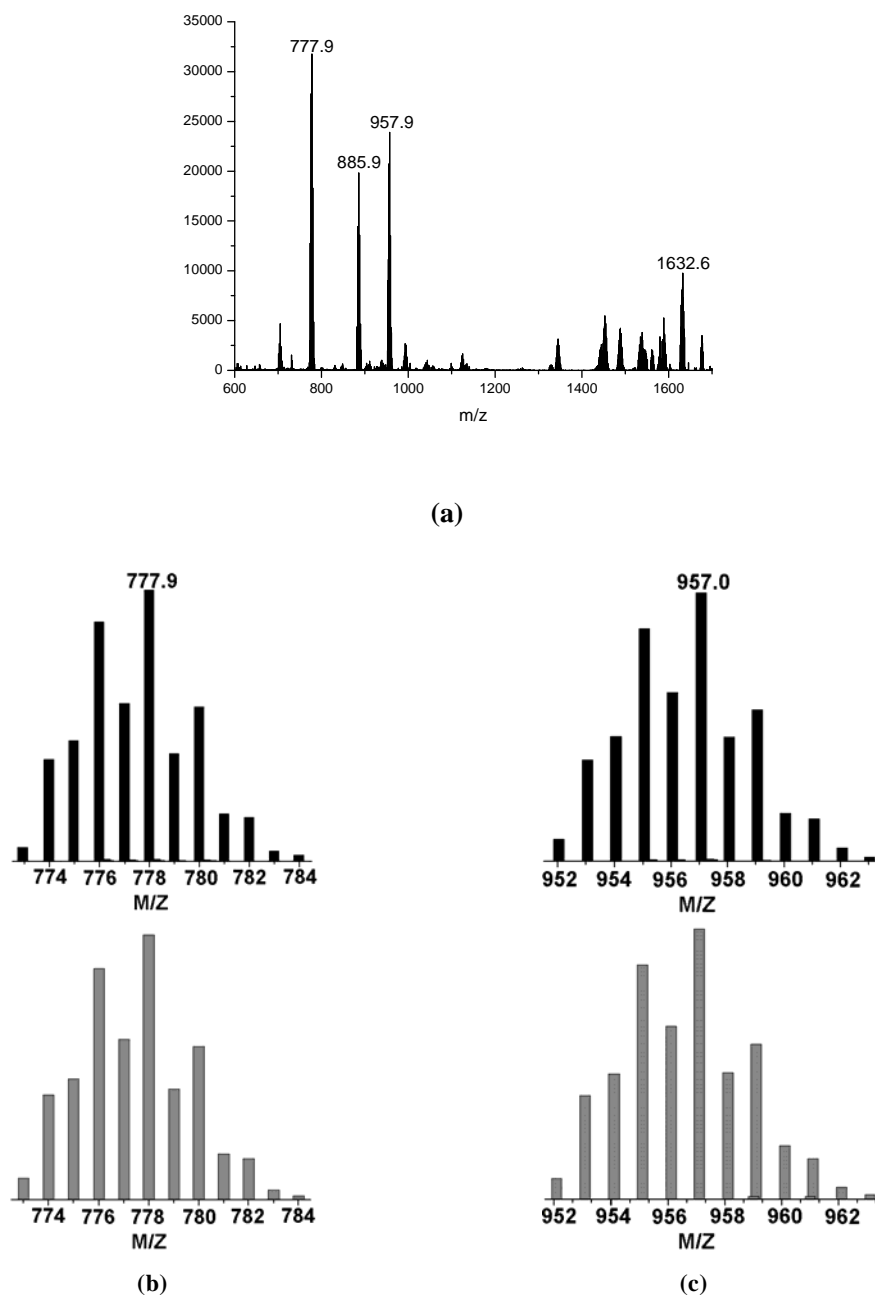
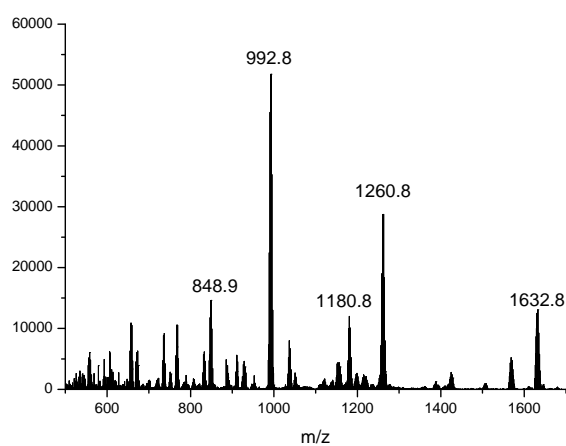
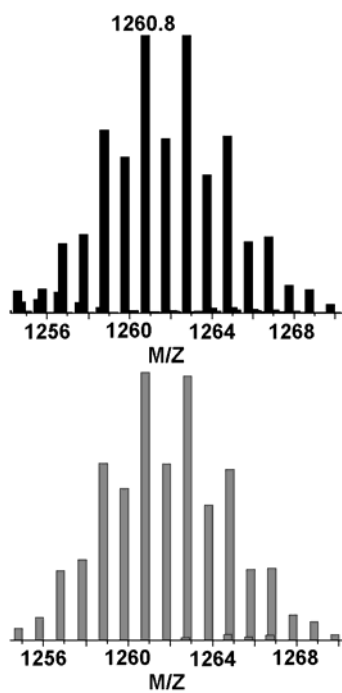


Figure S4. (a) The positive-ion ESI mass spectrum of **4** in DMF. (b) View of the observed (dark) and the calculated (gray) isotopic patterns for the $[\{\text{Tp}^*\text{WS}_3\text{Cu}_2\}+\text{DMF}]^+$ cation. (c) View of the observed (dark) and the calculated (gray) isotopic patterns for the $[\{\text{Tp}^*\text{WS}_3\text{Cu}_2(\text{MA})_2\}]^+$ cation.



(a)



(b)

Figure S5. (a) The positive-ion ESI mass spectrum of **5** in DMF. (b) View of the observed (dark) and the calculated (gray) isotopic patterns for the $[\{Tp^*WS_3Cu_3Br_3(MA)_2\}+2H]^+$ cation.

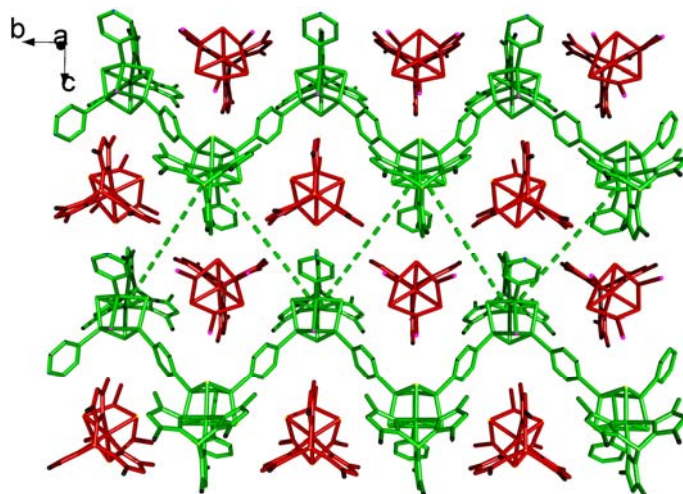


Figure S6. View of the arrangement of the cationic chain and the cluster anion of $3 \cdot \text{H}_2\text{O}$ along the *bc* plane.

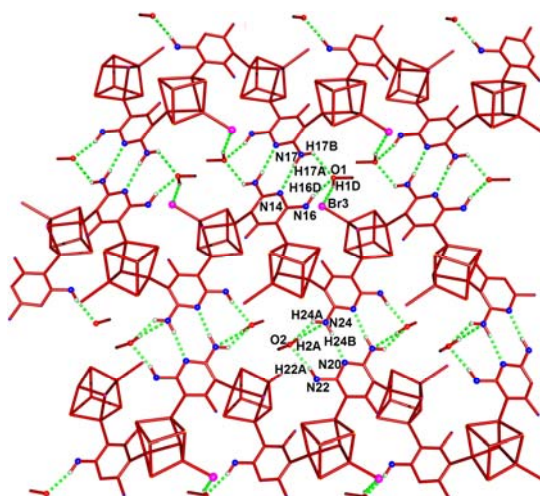
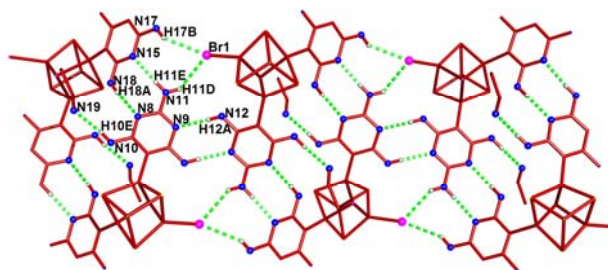
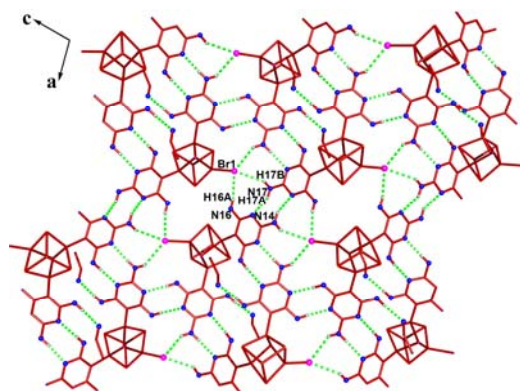


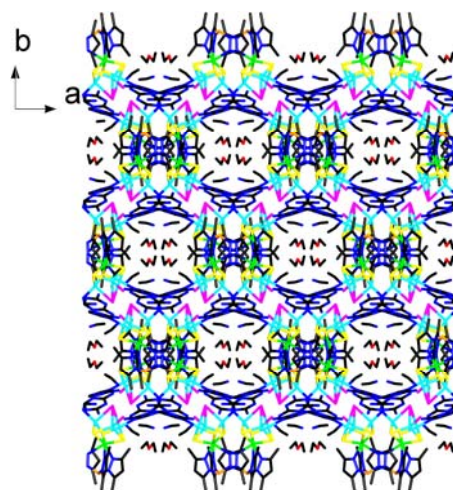
Figure S7. View of the 2D network derived from the hydrogen bonding interactions among the MA ligands and MeOH solvent molecules in $4 \cdot 2\text{MeOH}$.



(a)



(b)



(c)

Figure S8. (a) The H-bonding 1D chain in $5\cdot\text{MeCN}\cdot 0.5\text{Et}_2\text{O}$ extended along the c axis. (b) The H-bonding 2D network in $5\cdot\text{MeCN}\cdot 0.5\text{Et}_2\text{O}$ viewed along the ac plane. (c) The 3D H-bond structure in $5\cdot\text{MeCN}\cdot 0.5\text{Et}_2\text{O}$ looking down the c axis.

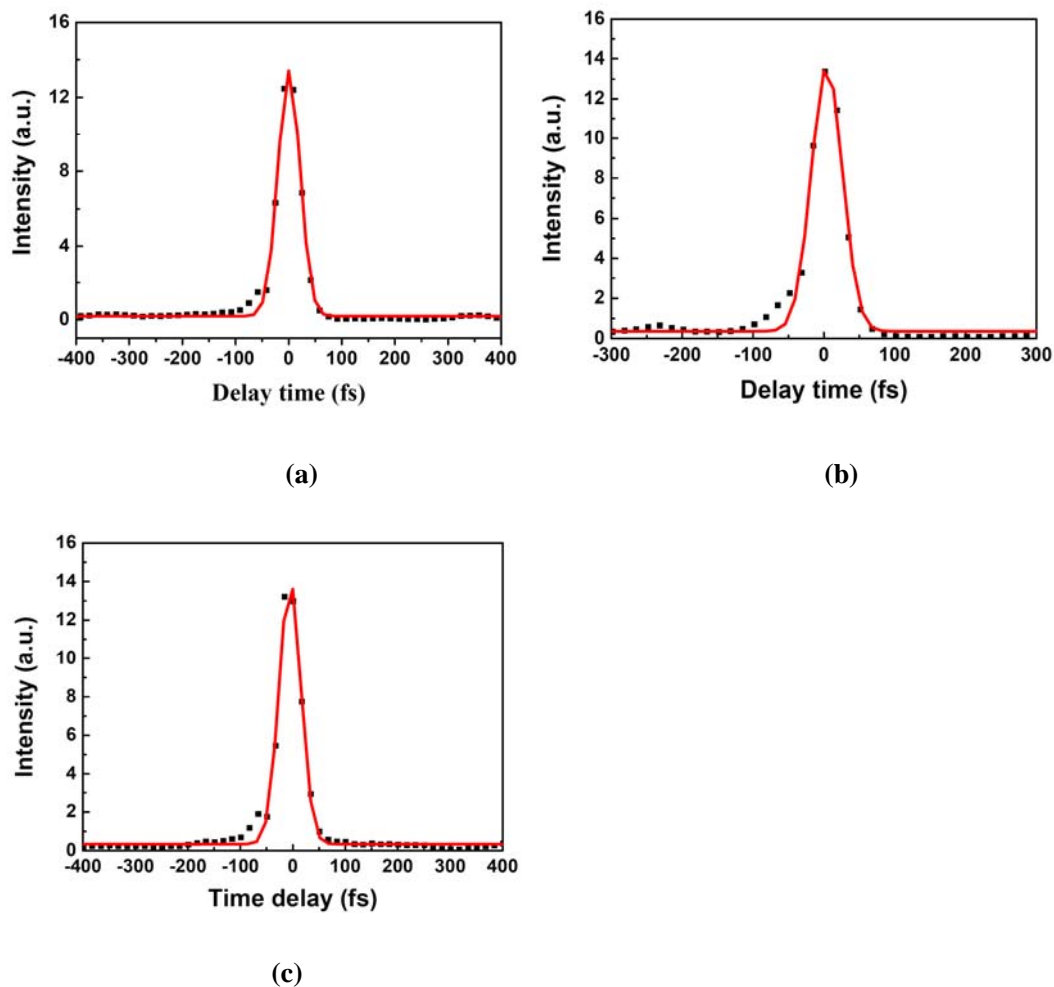


Figure S9. DFWM signal for the DMF solutions of **2** (a), **4** (b) and **5** (c) with concentrations 5.56×10^{-4} M for **2**, 2.75×10^{-4} M for **4** and 5.54×10^{-4} M for **5**. The black solid squares are experimental data, and the red solid curves are the theoretical fit.